



NEAR NET SHAPE FABRICATION VIA VACUUM PLASMA SPRAY FORMING

K.Balani¹, A.Agarwal¹ and T. McKechnie²

¹*Mechanical and Materials Engineering, Florida International University,
10555 W. Flagler Street, CEAS 3464, Miami, FL-33174, USA.*

²*Plasma Processes Inc., 4914 Moores Mill Road, Huntsville, AL 35811, USA*

ABSTRACT

Near net shape fabrication substantiates the manifestation of final structure near to the desired shape, therefore can easily cut down the price of finished product contributed by machining. Though conventional powder metallurgy techniques are prominent in fabricating near net shape structures with controlled porosity, it still lags in producing thin walled complex shapes with functionally graded/ differential structures. Hence, fabrication of complex near net shapes using Vacuum Plasma Spray (VPS) forming has emerged as innovative rapid prototyping technique for a variety of applications. In the present work, the nuances of near net shape fabrication by VPS technique have been explained. Few examples of spray formed structures such as hypereutectic aluminum-silicon, nanostructured aluminum oxide, and intermetallic iron aluminide thin sheet have been discussed. A detailed case study of VPS formed thin TaC structure for ultrahigh temperature application has been elucidated via near net shape fabrication.

1. NEAR NET SHAPE FABRICATION USING VPS FORMING

Owing to extreme brittle nature, conventional fabrication techniques find difficult to shape refractory materials and intermetallics into desired shapes. Moreover machining techniques incur extreme wastage of material and require dead time for the finishing of the structural component¹⁻³. Though few processes satisfy the near-net-shape fabrication criteria, a serious limitation is posed by the extreme melting points of refractory materials. Ultrahigh temperature material application range between 2500-3300 K and therefore the selection of crucibles to hold the melt and help to form the finished product becomes quite difficult.

Plasma spraying has been used as a versatile technique for depositing metals, alloys, polymers and ceramics as coatings⁴. Temperature in excess of 10,000 K are easily reached in the plasma flame, hence can melt any known material with great ease. With an impact velocity of 1-3 Mach, plasma sprayed structure depict a typical mechanically bonded layered structure. VPS utilizes HF (high-frequency) started, DC plasma to heat and accelerate powder feedstock for deposition onto negative shaped substrate/ mandrel for fabricating positive shape structure, Fig. 1. Generally Ar is used as the primary plasma gas with secondary He or H₂ gas for increased heat transfer. Plasma gun can be manipulated by computer control in six axes of motion. With the cooling rates usually observed in the range of 10³-10⁸ K/s, generation of ultrafine grain microstructure and non-equilibrium phases is not so surprising in the Vacuum Plasma Spray (VPS) formed structured⁴⁻⁶. Both metals and ceramics have been processed with densities exceeding 97% of theoretical densities^{2,3,7-9}.

Plasma gun and the mandrel are computer-controlled in VPS forming, hence fabrication of complex structures can be designed accordingly. Deposition rates can go as high as 20 lb/hr (9

kg/hr). Near net shapes, spray deposited onto preformed mandrel, help reduce the finish machining of the deposited structure. Removal of mandrel from the deposited structure hold a *critical importance* in the near-net fabrication of VPS formed structures. A comparison between VPS forming and conventional P/M processing route is schematically presented in Fig. 2, clearly showing high percentage of material getting wasted in conventional processing via grinding, pressing, and machining. Hence, VPS forming finds a vital usage in fabricating near net shape structures with minimized machining costs

A variety of materials and geometries namely hypereutectic metallic glass aluminum-silicon (commercially called Vanasil) ring, nanostructured aluminum oxide shell, intermetallic iron aluminide thin sheet, and ultra high temperature tantalum carbide cylinder have been near-net sprayed. Details of parts are given later in the paper.

2. SALIENT VPS PROCESSING VARIABLES

A variety of variables are involved in deciding the final properties of the VPS fabricated near net shape structures. Size and morphology of feedstock powder, gas velocity, standoff distance, mandrel temperature, spray current and voltage, substrate material, surface treatment, etc. are few among numerous parameters for tailoring the processing of near net shape structure. Few dominating parameters are described below:

2.1 Powder Feedstock: Powder size and morphology of feedstock powder is critical in deciding final microstructure and density of spray deposited structure. The most suited powder particle size distribution for VPS technique often varies between 15-45 μm . Fine powder ($<10 \mu\text{m}$) particles have tendency towards incoherent flow in hot plasma zone and result in overspray. On other hand, coarse ($>100 \mu\text{m}$) powder particles remain unmelted or get partially melted, resulting in subsequent structural porosity. Moreover, spherical powder morphology is the most suitable as it has good flowability, which is essential for consistent feeding during material deposition using spray forming technique.

2.2 Plasma Parameters: Plasma gun voltage, spray current and gas flow rates (primary and secondary) are the primary plasma parameters determining the degree of melting of the powder feedstock. Higher electrical power produces higher the degree of heat transfer to the powder particles, ensuring complete melting of powders. In conjunction with electrical power, primary gas (usually argon) flow rate determines the residence time of the powder particle in the plasma and the imparted kinetic energy. The degree of melting also depends upon the powder feed rate and thermal conductivity of the powder.

2.3 Mandrel material and design: The choice of mandrel material is very crucial for VPS forming of near-net structures. An ideal mandrel material should not react with deposited material, should withstand heat of plasma spraying and *should be easily separable from the deposited material*^{2,3,7-10}. Mandrel could be reused if non destructive methods such as cryogenic quenching is applied for separating it from deposited structure. Difference between the coefficient of thermal expansion (CTE) of mandrel and the spray deposited material is utilized to separate the mandrel. On the course, excess cooling could also lead to thermal shock therefore subsequent cracking in thin walled sprayed structures. Hence, controlling the degree of cooling is extremely critical in mandrel removal from near net shape fabricated structure. Graphite and 6061 aluminum have been used as mandrel materials for VPS forming.

3. EXAMPLES OF VACUUM PLASMA SPRAYED NEAR NET STRUCTURES

3.1 X-Ray Optics: Optical systems requiring extremely lightweight and stiff materials that should survive harsh thermal conditions are made from hypereutectic Al-Si (Vanasil) alloy. Bearing light-weight, temperature resistance, wear resistance and low CTE with better mechanical properties, applications of such material include windshield frames and structures in high speed aircraft, satellite mirrors, aircraft brakes, optical benches and gyroscopes, cylinder sleeves and piston rings for automobile engines. Preliminary investigations are done to fabricate 50 cm diameter, 5 cm high and 0.6-0.76 mm thick Vanasil ring for Solar X-Ray Imaging, Fig. 3. Suitable temperature range was identified for successful deposition and release of coating from 6061 Al mandrel^{7, 11}.

3.2 Iron Aluminide Sheets: Iron Aluminide is a candidate material for high temperature application due to its excellent sulfidation and oxidation resistance, low density, good wear and erosion resistance and potentially lower cost. Applications of this ordered intermetallic include high temperature structural material in fossil fuel energy plants, oxidation shields for tubes and incinerators in power plants, furnace fixtures and fasteners, hydroturbines, hot gas filters and heating elements. Poor ductility and inherent brittle nature of iron aluminide intermetallic restricts its fabrication into useful shapes. VPS forming of thin (150 μm) iron aluminide sheet, Fig. 4, demonstrates the capability of fabricating intermetallic thin sheets which could be easily rolled without any cracking¹².

3.3 Nanostructured Aluminum Oxide Shell: Researchers have been using depositions on small coupons or samples to study nanostructured coatings via plasma spray. However, there is no available literature details fabrication of bulk, freestanding nanostructured component by plasma spraying. Fig. 5 shows a novel VPS formed free-standing nanostructured alumina tapered cylindrical cones. These tapered cylindrical alumina shells have a wall thickness of 0.4-0.6 mm and were plasma spray formed using 6061 aluminum mandrel. Nanoalumina dispersed composites find a wide variety of applications including x-ray mirror shells and in electrical industry as arc tubes¹¹. Nano aluminum oxide reinforcements not only improve mechanical properties, but also the inside surface of the spray formed x-ray mirror shell. Hence both mandrel finish and alumina nanostructure contribute to the reflecting inner surface of near net shape fabricated x-ray mirror shell¹¹.

3.4 Vacuum Plasma Sprayed Near Net Shape TaC Structure: Fig. 6 shows the near net shape formed TaC cylinder with diameter of 25 mm and wall thickness of 2 mm. The near net structures, confirming closely to the specific application requirement, was sprayed onto a graphite mandrel via VPS forming. High temperature properties help generating higher specific impulse, reduce regenerative cooling, and increase thermal capability of material⁵. Hence, TaC as refractory material offers incentive for effective fuel-utilization increasing the temperature-limit and efficiency of the thermal protection systems, and high erosion-resistant thrusters.

4. CASE STUDY OF VPS FORMED TAC

High melting point (4153 K), good thermal conductivity (22 W/m/ K), high wear and erosion resistance under propulsion environment, low coefficient of thermal expansion (6.6×10^{-6} /K), high-temperature creep strength, thermal shock resistance, and high temperature thermal stability make Tantalum Carbide (TaC) very potential material for aerospace applications^{1,5,13-15}. TaC as refractory material offers incentive for effective fuel-utilization increasing the temperature limit thereby the efficiency of the thermal protection systems, high erosion resistant thrusters and nozzle throat inserts. Absence of much data in the literature guides our research towards characterization of ultra high temperature TaC ceramic via near net shape VPS forming.

4.1 TaC Powders: As-received TaC powder is very fine and ranged between 1-2 μm , with composition of 6.24 wt. % C, 0.1034 wt.% O_2 and rest Ta. Fine powders tend to clog the nozzle due to high interparticle friction and high surface area to volume ratio ^{2,4,16}. Spray drying helps towards better control of powder flow rate by agglomerating the powder particles into mass of spherical porous cake. Improved flow properties and reduced interparticle friction is clearly displayed by high magnification SEM images of spray-dried powder, Fig. 7.

4.2 Experimental Procedure: Vacuum Plasma Spraying was done using Ar primary gas and He as secondary gas under a vacuum of 75 - 200 torr for near net shape TaC forming. Scanning Electron Microscopy (SEM) has been carried out using JEOL JSM 5900LV electron microscope with integrated Energy Dispersive Spectroscopy (EDS) capabilities. X-ray diffraction (XRD) is used for phase identification and Transmission Electron Microscopy (TEM) is undertaken using FEI Tecnai F30 operating at voltage of 300kV.

4.3 Microstructure of VPS formed TaC: SEM micrograph, Fig. 8, elucidates various phases generated during the processing of VPS formed near net TaC structure. Variations of the contrast among phases indicate that diverse stoichiometries have been favored during the evolution of phases. Rapid solidification, inherent in the VPS forming, introduces non-thermodynamic cooling, which lead to exotic phase generation in the near-net shape structures.. Hence, extensive characterization is required for identifying different phases evolved during the VPS forming of near net shape TaC structure. Very fine and distributed porosity is seen in the microstructure and, as clear from the Fig. 8 micrograph, porosity is isolated and not interconnected. Surface polishing may show a higher degree of porosity because of peeling, since layer removal pulls off the splat particles beneath it. Density of VPS formed TaC was found greater than 92% of the theoretical density, depicting dense nature of splats as measured from water immersion technique.

4.4 Phase Analysis of TaC: Identification of various phases, generated in the VPS forming of near net shape TaC structure, are characterized by X ray diffraction (XRD). Fig. 9 depicts X-ray diffraction spectrum corroborates presence of Ta_2C during VPS forming of near net TaC structure. Confirmation of newly generated Ta_2C phase by XRD indicates that this phase is forming during the VPS forming. Presence of both TaC and Ta_2C phases is confirmed by XRD spectrum.

Free energy of formation for Ta_2C is lower than that of TaC, hence Ta_2C may be expected during the VPS forming of TaC near net structure ^{17,18}. The binary Ta-C phase diagram, depicts the tendency of Ta_2C to form a relatively low temperature eutectic (3116 K). Further research is being carried out to minimize Ta_2C phase by controlling the Ta/C ratio in the initial stoichiometry of powder and spray environment. It is important to stress during conventional processing that TaC readily oxidizes to form Ta_2O_5 as free energy of formation of Ta_2O_5 lies much lower than that of either TaC or Ta_2C . However, vacuum plasma processing avoided the formation of Ta_2O_5 .

4.5 Microhardness and Toughness Measurements: Vicker micro indentation methods are attractive methods for calculating the toughness of the material via radial cracks generated since residual stress of indentation get arrested when near tip stress intensity equilibrates with material's toughness. Semi-empirical relationship given by Kruzic and Ritchie to relate the

$$K_c = \chi \left(\frac{E}{H} \right)^{1/2} \frac{P}{a^{3/2}}$$

material toughness with the radial crack and material's hardness is expressed below¹⁹: where P is applied load, E represents Young's modulus, H values Vickers Hardness, a is radial crack, measured from center of indent, and χ is a calibration constant taken as 0.016 ± 0.004 . Vickers hardness observed in the normal to spray direction was measured in the range of 17.44 to 53.1 GPa. Carbon content, distribution of the phases, and the spray direction decide the Vickers hardness of the TaC sprayed structures. Radial cracks generated during the indentation were used to calculate the material toughness values of near net shape TaC structures along the normal spray direction. Toughness of spray formed structure stretched between 1.64-5.87 MPa m^{1/2} using the semi empirical formula given by Kruzic and Ritchie¹⁹.

4.6 TEM and High Resolution TEM Characterization: TEM image of an interface separating the distinguishable phases is clearly depicted in Fig. 10. Selected area electron diffraction (SAED) was used to characterize the crystal definition of generated phases. SAED analysis confirmed the existence of major stoichiometric TaC phase. High-resolution TEM image, Fig. 11, resolves the interplanar lattice spacing to excavate further details. The interface and the existing phases now are more clarified under the high resolution TEM image. To integrate crystallographic tools towards better understanding of the phase, CaRine 3.1 crystallographic software was used to create TaC and Ta₂C crystal structure with associated lattice parameters. Respective interplanar lattice spacing for various planes of these phases was calculated using a self-written computer program on Matlab 6.1 platform.

Generation of exotic metastable and non-stoichiometric phases is not uncommon for VPS formed TaC structure since rapid solidification processing produces phases not familiar to thermodynamic phase diagrams, and the corresponding lattice parameter of phases are earlier detailed by researchers²⁰⁻²².

High Resolution TEM image, Fig. 11, is categorized into various regions to throw light on the observation of different characteristics of the developed structure. Interface stands as conforming layer to accommodate the change between the phases on the either side to match the lattice spacings. The regions are divided into A, B, and C; where region B represents the interface. Region C represents lattice spacing of 2.70 Å corresponding to the crystallographic (100) plane of Ta₂C. Region A has a lattice spacing of 2.77Å, not matching with any interplanar spacing of TaC or Ta₂C crystal. Hence region A depicts non-stoichiometric phase generated during the VPS forming. Clarity of distinguishable non-stoichiometric phase confirms to the non-thermodynamic nature of the VPS forming. Generation of exotic phases direct the role of VPS forming parameters in deciding the final microstructure of the TaC near net shape structure.

5. CONCLUSIONS

It has been successfully shown that Vacuum Plasma spraying technique can be adopted for near net shape fabrication of difficult to process materials. Hypereutectic Al-Si (metallic glass) ring, Aluminum Oxide (nanostructured) shell, Iron-Aluminide (intermetallic) thin sheet, and Tantalum Carbide (ultra high temperature) cylinder have been near net VPS formed using Al 6061 and graphite mandrel. Non-thermodynamic Ta₂C phase generation was confirmed by XRD analysis, endorsing the formation of Ta₂C during the VPS forming. VPS forming optimization is further needed to reduce or avoid deleterious Ta₂C phase formation, which tends to form eutectic phase. Fracture toughness was measured between 1.64 and 5.87 MPa.m^{1/2} along the normal spray direction. Because of inherent rapid solidification nature of the process, transition of generating phases is accommodated by the interface.

6. ACKNOWLEDGEMENT:

Authors thank Plasma Processes Inc., Huntsville, AL, where the VPS formed near net shape structures were fabricated. Authors wish to thank Prof. S.Saxena and Mr. R.Gulve, CeSMEC, Florida International University, for facilitating XRD experiments. Authors extend sincere gratitude to Prof. S. Seal, and Mr. S. Patil, University of Central Florida for TEM Characterization. Authors thank Florida International University Foundation for extending facilities for this research.

7. REFERENCES:

1. K.Upadhyaya, J.M. Yang, and W.P.Hoffman, *The Am. Cer. Soc. Bull.*, (Dec. 1997), pp 51-56.
2. R.Hickman, T.McKechnie, and A.Agarwal, *37th AIAA/ ASME/ SAE/ ASEE/ Joint Propulsion Conference*.(8-11 July 2001, Salt Lake Utah).
3. A.Agarwal, T.McKechnie, S.Straett and M.M.Opeka, *Elevated Temperature Coatings: Science and Technology IV*, TMS (2001), pp 301-316.
4. T.Laha, K.Balani, B.Potens, M.Andara, A.Agarwal, S.Patil and S.Seal, *Surfaces and Interfaces in Nanostructured Materials and Trends in LIGA, Miniaturization and Nanoscale Materials*, TMS (2004), pp 103-112.
5. L.Trignan-Piot, M.Berardo, A. Charai, J.Gastaldi, and S.Giorgi, *Thin Solid Films* **248**, (1994), 12-17.
6. S.Sampath and H.Herman, *J. of Th. Sp. Tech.*, **5** (4), Dec. (1996), pp 445-456.
7. A. Agarwal, T. McKechnie and D. Engelhaupt, "Net Shape Forming of Light Weight Optical Structures for Space Applications", *Optics Manufacturing for Dual-Use*, Huntsville, AL, February 14-15, 2001.
8. A. Agarwal and T. McKechnie, "Spray formed Nano-grained Alumina Structures, *J. Thermal. Spray Tech.*, **12** (3), Sept. (2003), pp 350-359.
9. A. Agarwal, R. Hickman, T. McKechnie and J. S. O'Dell, "Advances in Near Net Shape Forming and Coating of Erosion Resistant Ultra High Temperature Materials" *Tri-Service Sponsored Symposium on Advancements in Heatshield Technology*, Huntsville, May 10-11, 2000.
10. A. Agarwal and T. McKechnie, "Spray Forming Aluminum Structures", *Advanced Mater. Process*, vol. 159 (5), 2001, pp. 44-46.
11. Agarwal and T. McKechnie, Low Cost Fabrication Lightweight Optics, Mirrors and Benches, NASA Goddard Space Flight Center, Technical Report NAS5-0008, November 2001.
12. Arvind Agarwal and Chris Power, "Near Net Shape Processing by Vacuum Plasma Spraying", PM2TEC 2002 World Congress, June 16-21, Orlando, Metals Powder Industries Federation, NJ.
13. L.Trignan-Piot, M.Berardo, J.Gastaldi, and S.Giorgio, *Surf. And Coat. Tech.* **79**, (1996), pp 113-118.
14. R.Teghil, L.D'Alessio, G.De Maria, and D.Ferro, *Appl. Surf. Sci.* **86**, (1995), pp 190-195.
15. L.Honeycutt III, W.H.Jennings and C.R.Manning Jr., *Wear* **37** (1976), pp 209-216.
16. L.L.Shaw, D.Goberman, R.Ren, M.Gell, S.Jiang, Y.Wang, T.D.Xiao, P.R.Strytt, *Surf. And Coat. Tech.* **130**, (2000), pp 1-8.
17. T.Ya. Kosalapova Ed., *Handbook of High Temperature Compounds: Properties, Production, Applications*. Hemisphere Publishing Corporation, (1990).
18. O. Kubaschewski, E. L. Evans, and C. B. Alcock, *Metallurgical Thermochemistry*, 4th ed., Oxford, New York, Pergamon Press (1967).
19. J.J.Kruzic, and R.O.Ritchie, *J. Am. Ceram. Soc.* **86** (8), (2003), pp 1433-1436.

20. M.W.Heaven, G.M.Stewart, M.A.Buntine, and G.F.Metha, *J. Phy. Chem. A* **104**, (2000), pp 3308-3316.
21. A.L.Bowman, T.C.Wallace, J.L.Yarnell, R.G.Wenzel, and E.K.Storms, *Acta Crys.* **19**, (1965), pp 6-9.
22. H.Wipp, M.V.Klein, and W.S.Williams, *Phy. Stat. Sol.(b)*, **108**, (1981), pp 489-500.

FIGURES

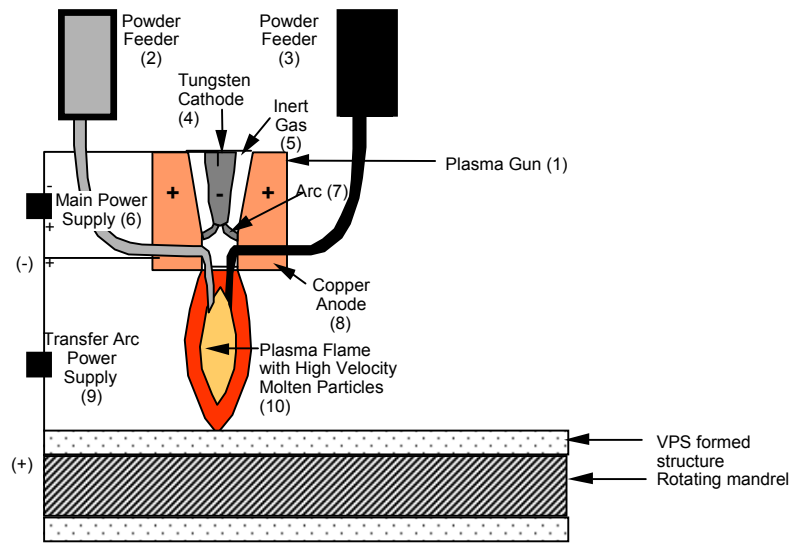


Fig. 1: Vacuum Plasma Spraying (VPS) processing showing rotating mandrel

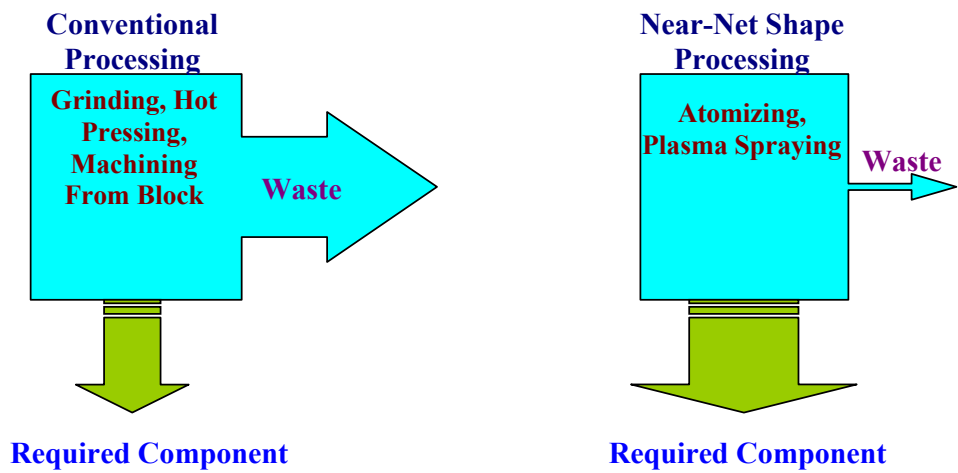


Fig. 2: Comparison between near net shape VPS forming and conventional P/M-processing.

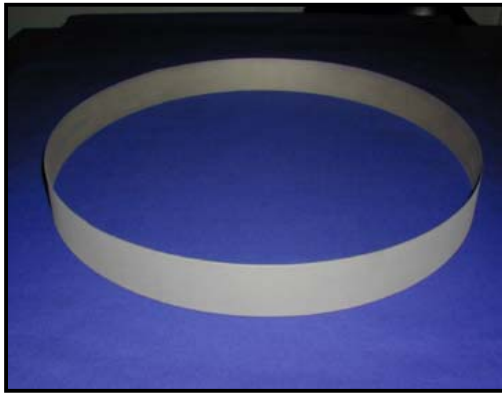


Fig. 3: A 50 cm diameter vanasil ring successfully deposited and released from a 6061 Al mandrel for making large mirrors by carrier shell approach.

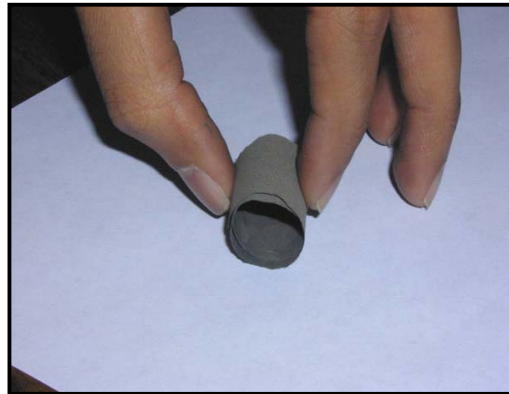


Fig. 4: Iron aluminide based intermetallic sheet (150 μm thick) fabricated by VPS technique. Thin sheet could be easily rolled without cracking.

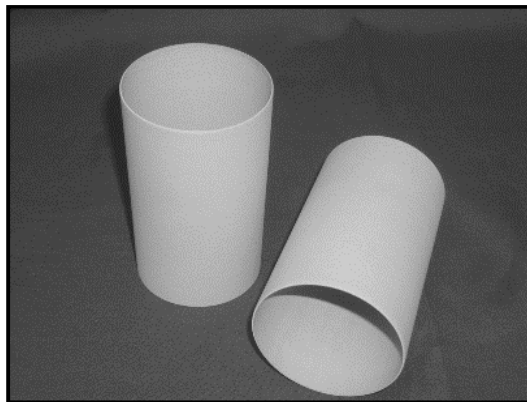


Fig. 5: Plasma spray formed nanostructured aluminum oxide shells with a wall thickness of 0.4-0.6 mm.



Fig. 6: Vacuum Plasma Sprayed Near Net TaC Cylinder

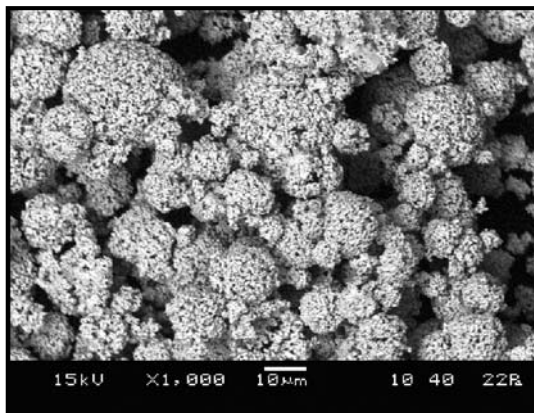


Fig. 7: SEM Micrograph of Spray Dried TaC Powder

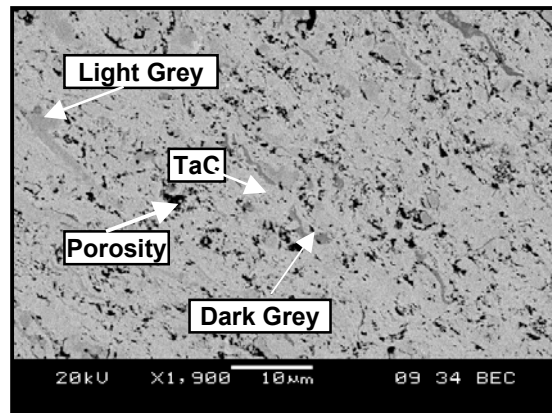


Fig. 8: SEM Micrograph of VPS Formed TaC Structure

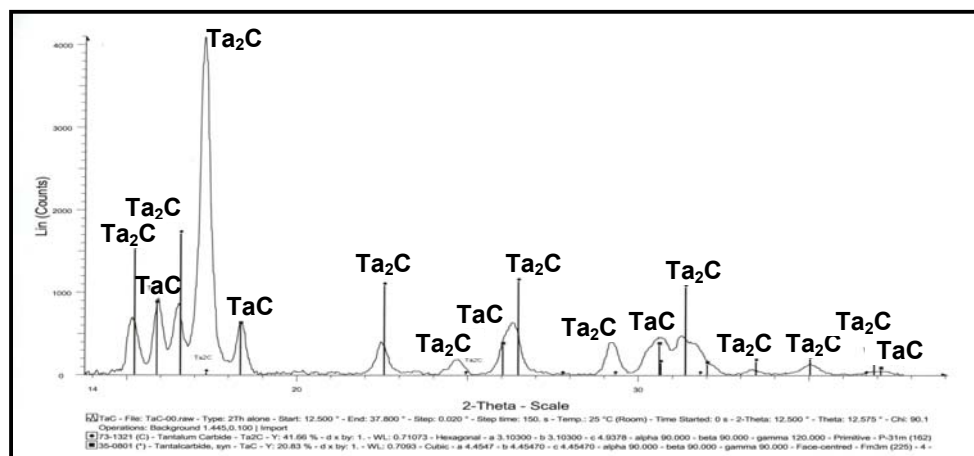


Fig. 9: X-Ray Diffraction Pattern for VPS TaC

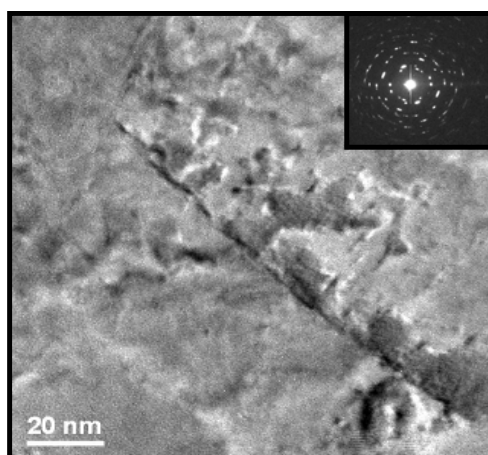


Fig. 10: TEM Image showing distinguishable phases

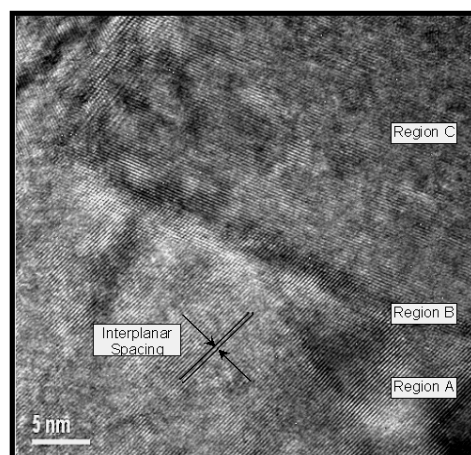


Fig. 11: High resolution TEM images displaying interplanar spacings and reaction zone